ACS APPLIED ELECTRONIC MATERIALS

pubs.acs.org/acsaelm

Article

Inkjet Printing of Aqueous Silver Inks on Water-Soluble Fabrics for Transient Electronics Applications

Zehra Gozutok Onses,* N. Burak Kiremitler, Aleyna Ozbasaran, Xian Huang, Mustafa Serdar Onses, and Hakan Usta*

Cite This: *ACS Appl. Electron. Mater.* 2024, 6, 5599−5607

Read Online

ACCESS | Metrics & More | Article Recommendations | Supporting Information

ABSTRACT: There is an urgent need to develop practical routes for manufacturing transient electronic devices to tackle the emerging issue of electronic waste and enable next-generation devices. This study reports additive patterning of conductive layers on industrially available water-soluble nonwoven fabrics composed of poly(vinyl alcohol) (PVA). Aqueous inks composed of reactive silver precursors can be practically patterned over water-soluble fabrics by inkjet printing. The efficient deposition of materials with droplet volumes on the order of picoliters ensures the generation of conductive patterns on a water-soluble fabric using a solution-processable fabrication with aqueous inks. The fabrication of conductive electrodes and transience behavior are studied on PVA fabrics with two different degrees of hydrolysis, providing tunability in the temperature-dependent degradation of the substrate. The application of the printed conductive pads is demonstrated in resistive heaters. The temperature of the fabric can exceed 100 °C in less than 15 s at a safe voltage of 3 V. The heater exhibits stable operation under cyclic heating and cooling. The presented approach presents key opportunities in additive patterning of aqueous solutions and colloidal dispersions over water-soluble substrates for transient device applications.

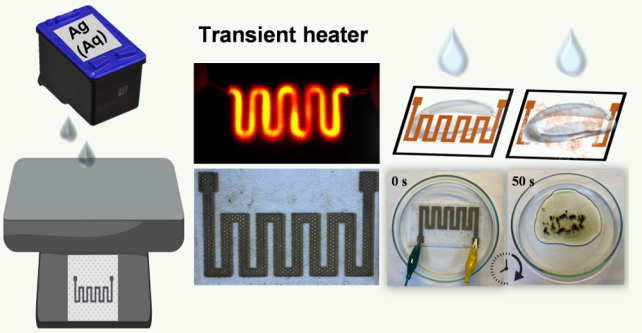

KEYWORDS: *transient electronics, inkjet printing, silver, poly(vinyl alcohol), electronic textiles, resistive heaters*

INTRODUCTION

The extreme digitization of the world in the current information age motivates a new generation of electronic systems. Unprecedented technological development over the past few decades has resulted in a significant amount of electronic waste, which poses serious environmental and health issues.[1] Considering that the typical service life of electronic devices spans only a few years, the management of electronic waste has become increasingly challenging and crucial than ever.[2] Furthermore, new forms of electronics devices are needed in emerging applications, such as temporary devices for diagnostics and therapeutics in biomedical applications. These devices should be safely disintegrated in the body, overcoming the need for additional surgeries to prevent associated infections and discomfort to patients. An emerging concept to address these pressing issues in the electronic waste management and new generation of applications is transient electronics.[3] Transient biomedical devices have been reported for continuous glucose monitoring,[4] energy harvesters,[5] brain sensors,[6] electronic stents,[7] and drug delivery devices.[8] Other applications for self-disappearing electronics include security chips,[9] energy storage devices,[10] and environmental monitoring sensors.[11] This unconventional form of electronics refers to controlled disintegration of materials and components via different mechanisms.[12] In certain cases, components disintegrate into biologically safe chemicals and enables biodegradable or bioresorbable electronics.[13] A range of different materials have been utilized in transient electronics applications.[14−17]

The patterning of conductive materials is essential for transient electronics applications. The water solubility of the substrates poses a practical challenge for the patterning process.[18] Direct utilization of conventional lithographic processes becomes impractical due to the excessive usage of solvents in multiple steps, such as spin-coating, development, and lift-off. As a result, the initial transient electronics demonstrations have relied on the physical vapor deposition of metals through stencil masks.[19] Other routes involved the fabrication of the necessary patterns on a donor substrate using conventional lithographic processes followed by solid-state transfer printing.[20] Laser-induced evaporation of metals was

Received: April 1, 2024
Revised: June 29, 2024
Accepted: July 15, 2024
Published: July 29, 2024

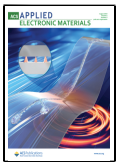

https://doi.org/10.1021/acsaelm.4c00569
ACS Appl. Electron. Mater. 2024, 6, 5599−5607

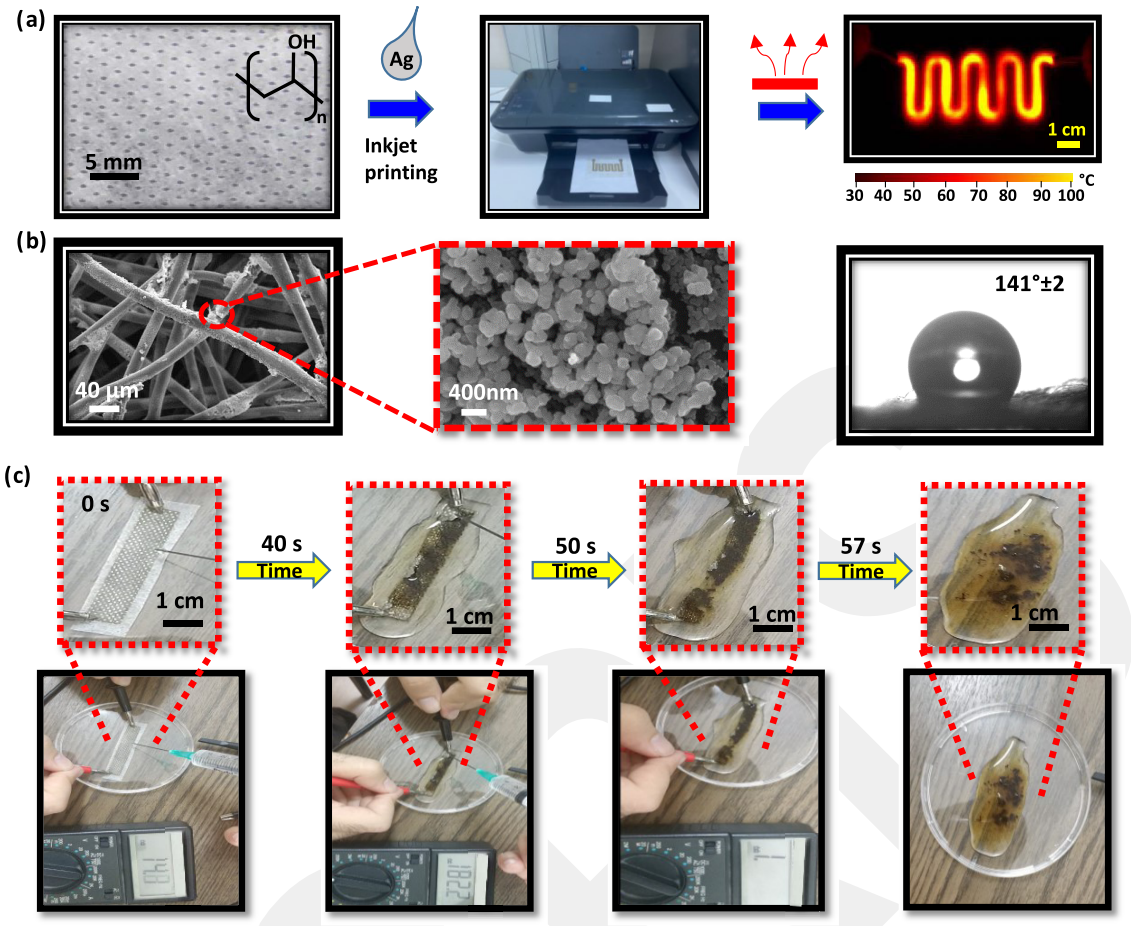

Figure 1. Inkjet printing of aqueous silver inks over PVA-based water-soluble fabrics for transient electronics applications. (a) Water-soluble fabric, inkjet printing particle-free silver ink, and a photograph showing an infrared camera image under a driving voltage. (b) SEM images of fibers (left) and silver particles (middle) that form after heating at 120 °C for 2 min; (right) photograph of a water droplet on the printed region along with the water contact angle. (c) Pictures taken over a minute upon exposure to water. The top row shows a pad printed with silver ink over the water-soluble fabric. The bottom row shows representative resistance measurements.

also utilized for the patterned transfer of metallic features.[21] These approaches have been instrumental for demonstrating the proof of the concept; however, they have limitations regarding mechanical placement of stencil masks and donor substrate, eventually leading to issues in terms of reproducibility, resolution, and practicality.

Solution-processing-based additive fabrication offers practical, low-cost, and rapid prototyping. Additive patterning techniques have attracted substantial interest in the practical manufacturing of electronics devices.[22] The contradicting requirements of solution processability of materials and solubility of the substrate are the key challenges, which greatly limit the applicable materials and methods. Most reports have used screen printing of materials dispersed in anhydrous solvents, which have been deposited on substrates via the use of stencil masks.[19,23,24] Drawbacks of this approach involve the need for a stencil mask and inefficient usage of materials, since large amounts of materials are deposited over the entire stencil mask. Furthermore, the need for paste-like inks requires the use of polymers, which impede effective electrical conductivity. Various forms of inkjet printing have attracted substantial interest in electronics applications.[25,26] The key advantages of such printing techniques involve the localized delivery of materials only to targeted areas in an efficient manner.[27] Although inkjet printing techniques are relatively mature, transient electronics applications have not benefited sufficiently from these advantages. The challenges for adaptability to transient substrates include clogging-related issues in printing of particle-containing inks and the use of solvents that can degrade the water-soluble substrates.

Herein, we present the fabrication of conductive patterns on water-soluble fabrics by inkjet printing of aqueous silver inks and demonstrate transient heaters. Unexplored for transient electronics applications, inkjet printing of particle-free and reactive silver inks is a versatile approach to generate conductive patterns. In this approach, a solution of silver precursors is printed, followed by a brief heating, which mediates the formation of metallic silver particles through a form of Tollens' process.[28] The issue of degradation of the substrate from the aqueous ink should be considered for the successful adaptation of this approach to water-soluble substrates for transient electronics applications: Efficient deposition of materials via inkjet printing in low volumes is key in addressing this issue and enabling the generation of conductive patterns on a water-soluble substrate. We use two different types of water-soluble nonwoven fabrics based on poly(vinyl alcohol) (PVA) as the substrate in this study. These fabrics are industrially available at a low cost and in large quantities, which favors adaptation in practical applications. The water solubility of PVA is determined by the intrinsic

https://doi.org/10.1021/acsaelm.4c00569
ACS Appl. Electron. Mater. 2024, 6, 5599−5607

properties[29] of the polymer such as the degree of hydrolysis (DH) and molecular weight, as well as structural parameters[30] such as the thickness. The DH from poly(vinyl acetate) is a convenient means of tuning the solubility of PVA in water.[31] With increasing DH, the water solubility of PVA decreases due to the enhanced hydrogen bonding between and within the polymer chains.[32] PVA materials with varying DH are commercially available at a low cost in nonwoven fabric forms, making them a viable choice for transient electronics applications. The utilization of two types of PVA fabrics presents options for degradation at room temperature and elevated temperatures. The dissolution process is studied with spectroscopic and structural characterization methods. Finally, we demonstrate transient wearable resistive heaters that have attracted increased attention recently for personal comfort and medical applications, where localized heating is exploited for pain management and wound healing.[33−35] Previously,[36] transient heaters were fabricated by spin-coating a film of water-soluble poly(L-lactic acid) (PLLA) on random networks of silver nanowires on poly(tetrafluoroethylene) substrate. PLLA films with the silver nanowires were then mechanically peeled off. The direct fabrication of transient heaters in a spatially tunable manner via inkjet printing will bring in new capabilities for varied applications. Thorough thermal characterization confirms the effective manufacturing of transient resistive heaters via inkjet printing of aqueous silver inks on water-soluble nonwoven PVA fabrics.

EXPERIMENTAL SECTION

Materials. Two types of nonwoven PVA fabrics were purchased from Goblen Inc. The Type-I fabric has a density of 30.4 g/cm^2 and dissolves rapidly in water at room temperature. The Type-II fabric has a density of 37.7 g/cm^2 and dissolves in water at elevated temperatures. Silver acetate (Sigma-Aldrich), formic acid (95%, Sigma-Aldrich), and ammonia solution (25%, Merck) were used to prepare the ink.

Preparation of Particle-Free Silver Inks and Printing. The synthesis of particle-free silver inks followed the literature with minor modifications.[28,37] In a typical synthesis, 1 g of silver acetate was dissolved in 2.5 mL of ammonia solution for ∼10 s, followed by the slow addition of a solution of formic acid with a volume of 0.2 mL. To remove the large particles, centrifugation was performed at 4000 rpm for 30 min. The supernatant was used as the ink for printing on water-soluble nonwoven fabrics. An inkjet printer (HP Deskjet Ink Advantage 2060) was used for patterned deposition of the ink. The cartridges were thoroughly washed in ethanol multiple times until the clear solution flowed out of the nozzles. The synthesized ink was loaded in a volume of ∼1 mL to the cartridge. Inkjet printing was performed with a setting of 720 dots per inch. To generate sufficiently conductive features, printing was repeated five times. Upon printing, the substrate was heated at 120 °C for 2 min on a hot plate. The dissolution of the fabrics was performed by immersing the fabrics in a beaker filled with tap water.

Characterization. The morphology of the fabric and printed inks was characterized by scanning electron microscopy (SEM, Zeiss EVO LS10, 25 kV). Energy-dispersive X-ray (EDX) spectroscopy (Bruker) attached to the SEM was preferred to analyze the chemical composition of the samples. Fourier transform infrared spectroscopy (FTIR, PerkinElmer 400) and Raman spectroscopy (WITec α 300 M + confocal, 532 nm laser) were used to probe the chemical composition of the two types of fabrics. The static water contact angle of the nonwoven sample was measured by means of a contact angle meter (Attension, Theta Lite). The resistances of the printed electrodes were measured by the four-probe technique using a multimeter (Keithley 2450). For demonstration purposes, the resistances were also measured by the two-probe technique using a digital multimeter (EDM-168A—Escort). To perform the resistive heating experiments, a DC bias of varied voltages was applied via a power supply. The electrical contacts were made by directly attaching crocodile clips to the printed electrodes. The temperature of the transient fabrics was measured by means of an infrared camera (Fluke TIS75). The focusing distance was approximately 15 cm, and the IR emissivity value was set to 0.95. The photograph of the measurement setup is given in Supporting Figure S1.

RESULTS AND DISCUSSION

Figure 1 presents the essential fabrication steps and the key results regarding inkjet printing of aqueous silver inks on water-soluble fabrics for transient electronics applications. In this study, two types of PVA-based nonwoven fabrics serve as substrates with a tunable water solubility characteristic, and silver-based conductive pads are deposited by inkjet printing of particle-free solutions of reactive precursors. This ink composition facilitates clogging-free printing, and the solid, conductive silver patterns form upon mild heating. The ability to deposit an aqueous ink onto a water-soluble substrate is made possible by depositing minimal ink volumes, thus minimizing the contact duration between the liquid and solid substrate phases. It is clear that the enhanced evaporation rates of liquids from low-volume droplets having large surface area-to-volume ratios contribute to this phenomenon.[28,38] Otherwise drop-casting of the same ink with a volume on the order of microliters immediately dissolves and damages the water-soluble fabric (Supporting Figure S2). The substrate was heated at 120 °C for 2 min immediately after the inkjet printing process, which thermally initiated reactions for on-site formation of silver particle patterns on the water-soluble fabric (Figure 1a).[28] The fabricated patterns exhibit high conductivity, facilitating their use in resistive heaters. Here, it is noteworthy that this pattern layout can be easily controlled using computer-aided design, similar to the software used in office inkjet printers. Figure 1a shows an example of a geometry (Supporting Figure S3) composed of linear features. Infrared camera imaging confirmed the effective heating of the entire pattern. SEM imaging confirms the formation of silver particles with high density, providing a continuous pathway for electrical conduction. Upon printing and annealing, the formation of silver particles on the fabric's fibrous morphology leads to a hydrophobic surface with a contact angle of ∼141°. Such a high contact angle is a result of air pockets that form between the water droplets and solid substrate.[39] This hydrophobicity enhances the stability of the printed electrodes against humidity and water during postprocessing and operation. Upon exposure to water, the fabric starts to dissolve, resulting in disintegration and vanishing of the conductive features. The DH provides tunability of the fabric's aqueous dissolution properties. While Type-I fabric can easily dissolve in water at room temperature, Type-II fabric requires elevated temperatures for dissolution. Figure 1c shows a series of photographs taken over time upon placement of water droplets on top of the printed electrodes on Type-I fabric. Within the first 30 s of exposure to water droplets, the electrical conductivity can still be measured, thanks to the hydrophobicity of the printed regions. When water droplets reach the unprinted regions, the fabric rapidly dissolves, and within a minute, the entire printed electrode disintegrates and exhibits a transient behavior (see Supporting Video S1 for the disintegration process).

https://doi.org/10.1021/acsaelm.4c00569
ACS Appl. Electron. Mater. 2024, 6, 5599−5607

The conductivity of the printed pads on water-soluble fabric can be gradually enhanced with repeated inkjet printing over the same region. Table 1 presents the sheet resistance of the printed pads for a varied number of printing layers. The sheet resistance decreases with the increasing number of printing layers, reaching as low as 2.6 Ω/square for Type-I and 2.1 Ω/square for Type-II fabrics after 5 layers. These findings are in agreement with the previous reports,[40,41] which have demonstrated similar trends and sheet resistance values for printing reactive silver inks on flexible, nontransient substrates. The need for repeated number of layers can be circumvented by tuning the printing conditions yielding a higher flow rate of materials.[42] In the case of printing aqueous inks over water-soluble fabrics, restricting the unit volume of materials per deposition, especially for the first layer, is advantageous to prevent substrate dissolution. After the first layer, the printed region becomes highly hydrophobic, and this hydrophobicity remarkably enhances the stability of the underlying water-soluble fabric. We note that this approach may open up varied opportunities for further incorporation of functional materials dissolved/dispersed in water onto water-soluble fabrics.

Table 1. Sheet Resistance (Ω/Square) of Printed Pads on Water-Soluble Fabrics for Varied Number of Printing Layers

	1 layer	2 layers	3 layers	4 layers	5 layers
type-I		42.8 ± 8.2	9.7 ± 4.2	4.9 ± 2.1	2.6 ± 0.7
type-II		44.6 ± 9.5	11.6 ± 4.9	4.6 ± 2.0	2.1 ± 0.6

To tune the dissolution behavior, we used two types of nonwoven PVA fabrics. Figure 2 presents the Raman and FTIR spectra of these fabrics. The Raman spectra (Figure 2a) for both types of fabrics exhibit characteristic bands that are in good agreement with the literature.[43] The strongest band observed at ∼2911 cm^{-1} is associated with the stretching vibrations of the CH_2 groups present on the polymer backbone. Vibrations of CH and OH appear at around 1430 and 1175 cm^{-1}, respectively. On the other hand, the FTIR spectra (Figure 2b) display characteristic bands such as O−H stretching (3240 cm^{-1}), CH_2 asymmetric stretching (2914 cm^{-1}), and CO stretching (1141 cm^{-1}), which align well with the literature.[44,45] A key difference between the two types of fabrics can be observed near 1750 cm^{-1}, which is associated with C═O remaining from the poly(vinyl acetate).[46] The lower the intensity of this band, the higher the DH value. Type-II fabric has a higher DH with the corresponding band being weaker. Higher DH leads to lower solubility due to the strong hydrogen bonding interactions between the PVA chains. The absorption band at 1141 cm^{-1} is particularly sensitive to the crystallinity of PVA.[44] The decrease in the crystallinity of Type-I fabric contributes to its higher water solubility in comparison to that of Type-II fabric. Figure 2c shows a schematic for highly plausible hydrogen bonding interactions between the PVA polymer backbone and water molecules, which, in turn, affects the polymer's water solubility. The polar hydroxyl (−OH) groups of PVA tend to bind with the polar water molecule, with each −OH bond being bound by two polar water molecules from the weak -H bond.

Upon printing of reactive silver inks and thermal annealing, highly conductive patterns form on the water-soluble nonwoven fabrics. Figure 3 presents the morphological and chemical characterizations of the silver particles on water-soluble nonwoven fabrics. SEM images (Supporting Figure S4) of the bare fabric show a highly interconnected morphology having randomly positioned fibers and bonding regions. This morphology results from the conventional nonwoven fabric manufacturing process. Upon printing the ink and thermal annealing, silver particles form over the fibers and bonding regions for both types of nonwoven PVA fabrics (Figure 3a,b). The formation of silver particles with a high surface coverage ensures an interconnected network for efficient electrical conductivity, as is evident from the SEM images at high magnification. While the EDX spectrum (Figure 3c) confirms the presence of silver element within the printed regions, mapping (Figure 3d) confirms that the density of silver particles is higher over the bonding regions in comparison to the fibers. The silver particles particularly formed on the bonding regions with a high density, likely due to their flat nature. XRD diffraction pattern (Figure 3e) confirms the formation of metallic silver with its diffraction peaks located at 2θ = 38.4, 44.3, 64.4 and 77.4°, which refer to characteristic planes of the face-centered cubic crystal structure.

The dissolution characteristics of the conductive patterns printed on two types of water-soluble fabrics were also studied. Conductive pads measuring an area of 5 × 1 cm^2 were printed over a fabric, which has a size of 6 × 1.5 cm^2. Figure 4 presents the time-dependent resistance of the printed conductive patterns that are exposed to water droplets at two different temperatures (25 and 60 °C). Water droplets were consistently

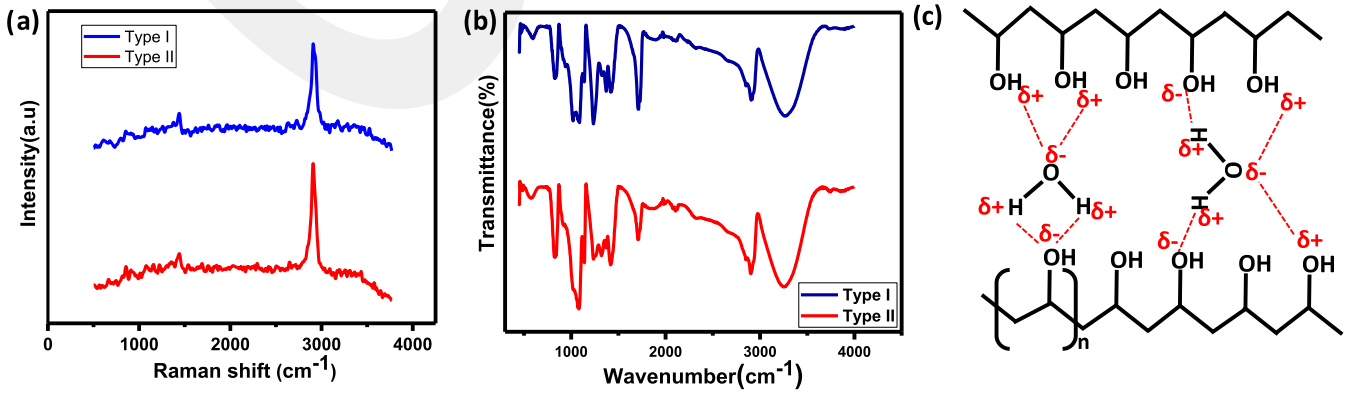

Figure 2. Characterization of water-soluble nonwoven fabrics. (a) Raman spectra, (b) FTIR spectra, and (c) hydrogen bonding-based interaction between PVA chains and water molecules.

https://doi.org/10.1021/acsaelm.4c00569
ACS Appl. Electron. Mater. 2024, 6, 5599−5607

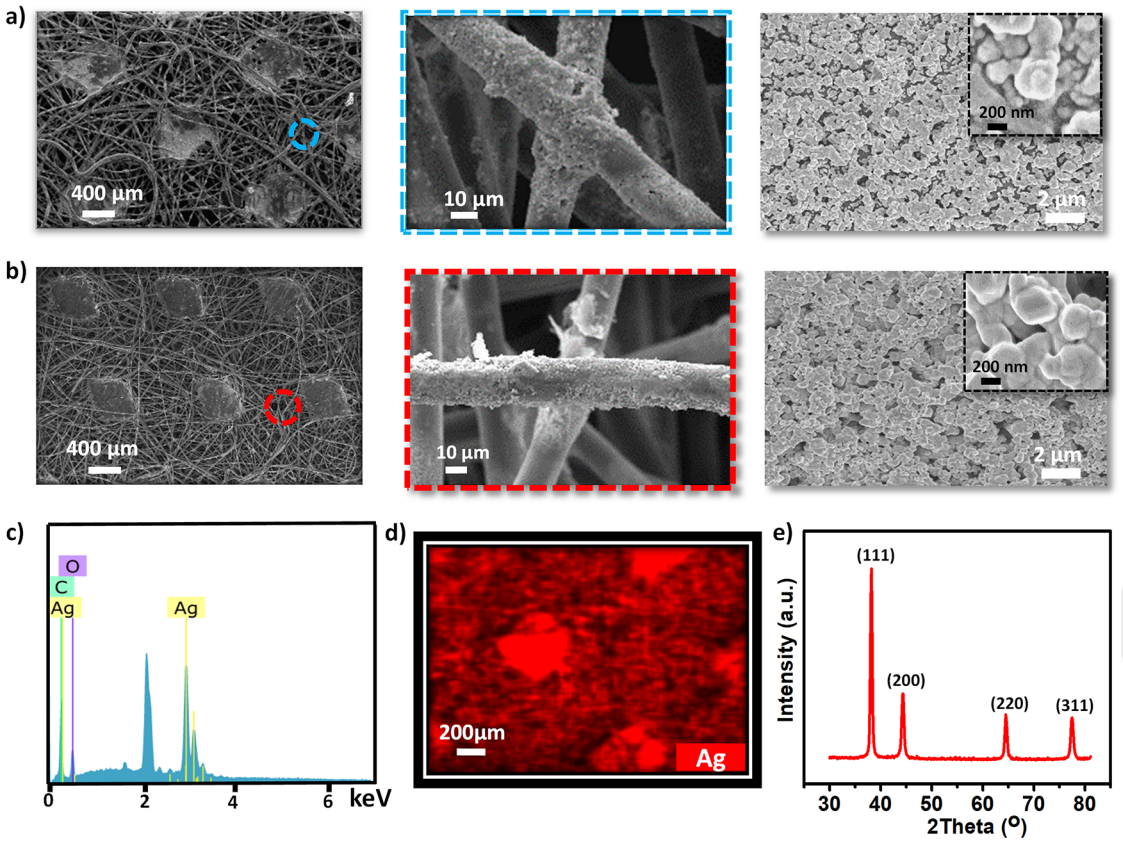

Figure 3. Structural and chemical characterization. (a, b) SEM images of the nonwoven fabric after printing and thermal annealing for (a) Type-I and (b) Type-II. (c) EDX spectrum, (d) EDX mapping image, and (e) XRD diffraction pattern for silver pads printed on Type-I fabric.

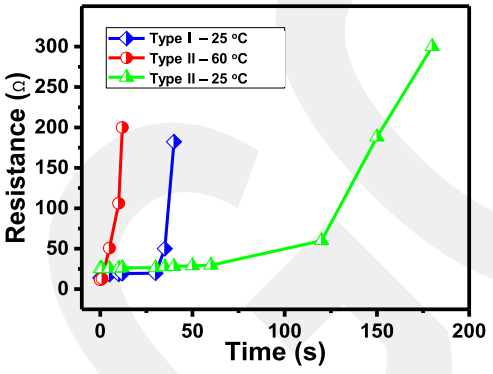

Figure 4. Transience behavior of conductive pads printed on two types of PVA-based fabrics.

dispensed onto the conductive pads using a syringe. The high hydrophobicity with a water contact angle of 141° (Figure 1c) delayed the interaction of water droplets with the underlying water-soluble fabric. When treated with room-temperature water, the conductive patterns on Type-I fabric begin to disintegrate after 30 s and a significant increase in the resistance was observed. No resistance measurements could be taken after 40 s exposure to water droplets at room temperature, and approximately after 50 s, the sample was completely disintegrated for Type-I fabric. For the Type-II fabric, the printed pads maintained conductivity for an extended duration when exposed to room-temperature water droplets. This result is attributed to the chemical differences between the two types of fabrics, as discussed above. The resistance increased up to approximately 3 min, beyond which no measurement could be taken, and the sample shrank and remained intact (Supporting Figure S5). However, at a water temperature of 60 °C, Type-II fabric with the conductive pad completely disintegrated within a much shorter time, typically on the order of several seconds. Collectively, these results confirm the transient behavior of our conductive electrodes fabricated on water-soluble fabrics. The dissolution can be tuned by the intrinsic properties of the fabric, as well as the water temperature. The humidity of the working environment can affect the performance of devices due to the swelling of PVA to an extent that depends on the type of fabric. Encapsulation layers[18] can be employed to improve the stability of devices.

The printed conductive patterns on the water-soluble PVA fabrics exhibited a high temperature and bending stability. First, the nonwoven PVA fabrics were subjected to temperatures ranging from 40 to 100 °C for 500 s (Supporting Figure S6). The printed electrodes remained conductive throughout this temperature range and exhibited a resistance increase less than 0.1 Ω for both types of fabrics. The very limited variation in the conductivity implies a sufficient level of thermal stability. Another important aspect of our current approach for flexible substrates is their mechanical stability under repeated deformation. To probe the mechanical stability, we adapted a cyclic bending test that is commonly used for flexible electronics. The electrodes printed on the fabrics remained conductive after 1000 cycles of bending to a radius of curvature of 6.5 mm (Supporting Figure S7). The resistance showed less than 2 Ω of increase after 1000 bending cycles for both types

https://doi.org/10.1021/acsaelm.4c00569
ACS Appl. Electron. Mater. 2024, 6, 5599−5607

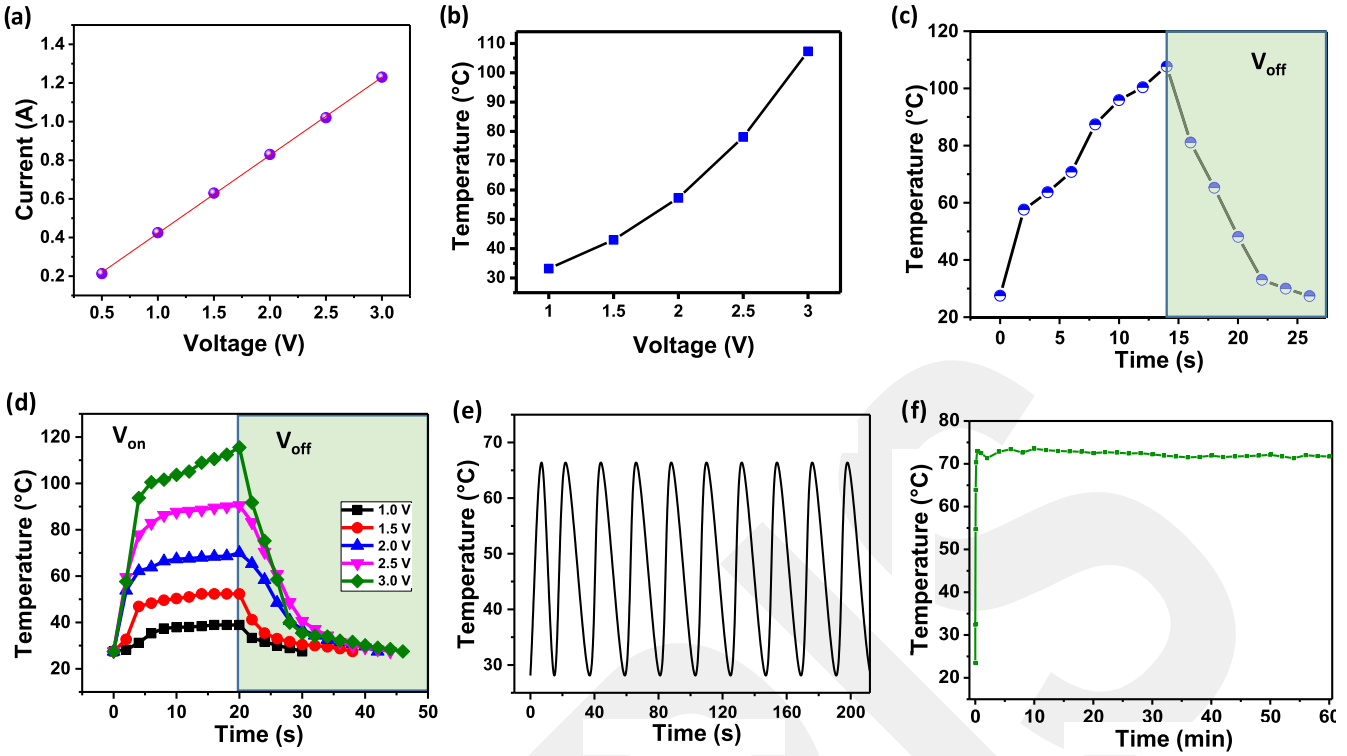

Figure 5. Resistive heating characteristics of transient electrodes fabricated by inkjet printing aqueous silver inks on Type-I PVA fabric. (a) Current−voltage curve, (b) temperature−driving voltage curve, (c) electrical heating for 15 s and natural cooling behavior at a driving voltage of 3 V, and (d) electrical heating for 20 s and natural cooling behavior at multiple driving voltages. (e) Cyclic heating and cooling curves at a driving voltage of 2 V. (f) Temperature stability for a constant driving voltage of 2 V. The temperature values represent the peak temperatures achieved during resistive heating.

of fabrics. Note that almost half of the resistance increase was recovered after a short (~30 s) standby time after the bending cycles. Collectively these experiments suggest a sufficient level of stability for the conductive patterns fabricated on water-soluble fabrics.

Finally, we demonstrate an application in transient heaters. Wearable electrical heaters function by producing heat through the flow of an electric current. Commonly referred to as Joule, resistive, and Ohmic heaters, they find applications in personalized heating, thermotherapy, and wound healing. Figure 5 shows the characteristics of transient electrical heaters in a rectangular geometry with dimensions of 4 × 1 cm^2 prepared by inkjet printing of reactive silver inks. The current−voltage relationship is linear[47] (Figure 5a), verifying the high conductivity of the printed electrodes on water-soluble fabrics. Figure 5b and Supporting Figure S8 show the temperature of fabrics and temperature mapping images obtained via an infrared camera for varied driving voltages, respectively. The temperature increases in response to an increase in the voltage. At a relatively small voltage of 3 V, the fabric can reach a high temperature of 107.6 °C. The heating efficiency, indicated by the slope of the maximum temperature achieved relative to the power density (Supporting Figure S9), was calculated as 91 ± 4.2 °C cm^2/W. The low-voltage heaters provide a safe and efficient option for wearable applications.[48] Furthermore, such low driving voltages provide the possibility to power the heater via flexible energy storage[49] and energy generator[50] systems. Temperature mapping images showed that the entire printed region exhibited a uniform distribution implying for the homogeneous printing of the ink and generation of conductive silver over the water-soluble fabric. A rapid heating−cooling behavior is highly desired for varied applications. Figure 5c shows time-dependent heating and cooling behavior at 3 V. The temperature can exceed 100 °C in less than 15 s and cools to room temperature in ~10 s. This result implies efficient transmission of electrical energy to heat energy by means of resistive heating. Further experiments demonstrate the tunability of the temperature and cyclic stability of the presented platform. The applied voltage bias directly determines the temperature of operation (Figure 5d). By increasing the driving voltage from 1 to 3 V, the temperature can be tuned from room temperature to 100 °C. In all cases, the desired temperature can be reached rapidly followed by immediate cooling when the voltage was turned off. The rapid cooling ensures safe operation in wearable applications. The stable operation of the heater is vital for wearable heater applications. Figure 5e shows the cyclic heating and cooling behavior of transient heaters fabricated by inkjet printing aqueous silver inks on a water-soluble Type-I PVA fabric. The voltage provided by a DC power supplier was turned on and off in a cyclic manner. This graph confirms the repeatable good heating stability of the conductive printed fabric heater. Additionally, the long-term stability of the heating/cooling performance is evaluated by performing 300 heating/cooling cycles under 2 V voltage. This confirms that the same heating/cooling behavior was observed throughout the long-term stability tests. There was no distorting or deformation in the fabrics as a result of repeated heating and cooling cycles. The fabric can maintain a steady-state temperature for extended periods of time (Figure 5f). There is a slight increase in the resistance of the electrode due to the temperature elevation associated with in situ heating (Figure S10). The maximum

https://doi.org/10.1021/acsaelm.4c00569
ACS Appl. Electron. Mater. 2024, 6, 5599−5607

variation in the resistance accounts for ~4% in the heating up and remains less than 1% in the steady-state plateau region indicating the operational reliability of the heater. The power density increased with the driving voltage and was 0.4 W/cm^2 at 2 V. Achieving such power densities requires higher driving voltages for carbon nanomaterial-based electrical heaters.[51]

CONCLUSIONS

This manuscript reports a counterintuitive approach based on inkjet printing of aqueous silver inks over water-soluble nonwoven fabrics for transient electronics applications. The minimal contact with liquids during the printing of inks at low volumes plays a key role in this approach. Upon printing the reactive silver ink and thermal annealing, silver particles form on the surface of the water-soluble fabrics with high conductivity. The strong hydrophobicity of the printed patterns further contributes to the stability of the fabrics against exposure to water. Industrially available low-cost PVA fabrics with different water solubility characteristics enhance options for degradation and disintegration of the functional units. The reported approach expands the solution-processable fabrication of transient electronics devices and components. Future works can explore other functional materials deposited by inkjet printing. The hydrophobic silver layer can also serve as a seed for the growth/deposition of materials with additional functionalities, such as photocatalytic activity, antimicrobial properties, electrochemical activity, and photoluminescence.

ASSOCIATED CONTENT

Supporting Information

The Supporting Information is available free of charge at https://pubs.acs.org/doi/10.1021/acsaelm.4c00569.

Disintegration of electrodes printed on the fabric upon exposure to water droplets (Video S1) (MP4)

Photographs of water-soluble nonwoven fabrics following drop-casting aqueous silver inks, additional SEM images, degradation of a conductive pattern on Type-II fabric, and temperature and bending stabilities of printed electrodes (PDF)

AUTHOR INFORMATION

Corresponding Authors

Zehra Gozutok Onses − *Department of Nanotechnology Engineering, Abdullah Gül University, 38080 Kayseri, Turkey*; Email: zehragozutk@gmail.com

Hakan Usta − *Department of Nanotechnology Engineering, Abdullah Gül University, 38080 Kayseri, Turkey*; orcid.org/0000-0002-0618-1979; Email: hakan.usta@agu.edu.tr

Authors

N. Burak Kiremitler − *ERNAM—Nanotechnology Research and Application Center and Department of Materials Science and Engineering, Erciyes University, Kayseri 38039, Turkey*; orcid.org/0000-0001-6065-4899

Aleyna Ozbasaran − *ERNAM—Nanotechnology Research and Application Center and Department of Materials Science and Engineering, Erciyes University, Kayseri 38039, Turkey*

Xian Huang − *Department of Smart Sensing, Tianjin University, Tianjin 300072, China; State Key Laboratory of Precision Measuring Technology and Instruments, Tianjin University, Tianjin 300072, China*; orcid.org/0000-0002-8788-9185

Mustafa Serdar Onses − *ERNAM—Nanotechnology Research and Application Center and Department of Materials Science and Engineering, Erciyes University, Kayseri 38039, Turkey*; orcid.org/0000-0001-6898-7700

Complete contact information is available at: https://pubs.acs.org/10.1021/acsaelm.4c00569

Notes

The authors declare no competing financial interest.

ACKNOWLEDGMENTS

This work was supported by TUBITAK under grant no. 122C168.

REFERENCES

(1) Hsu, E.; Barmak, K.; West, A. C.; Park, A.-H. A. Advancements in the treatment and processing of electronic waste with sustainability: a review of metal extraction and recovery technologies. *Green Chem.* **2019**, *21* (5), 919−936.

(2) Fu, K. K.; Wang, Z. Y.; Dai, J. Q.; Carter, M.; Hu, L. B. Transient Electronics: Materials and Devices. *Chem. Mater.* **2016**, *28* (11), 3527−3539.

(3) Hwang, S.-W.; Tao, H.; Kim, D.-H.; Cheng, H.; Song, J.-K.; Rill, E.; Brenckle, M. A.; Panilaitis, B.; Won, S. M.; Kim, Y.-S.; et al. A physically transient form of silicon electronics. *Science* **2012**, *337* (6102), 1640−1644.

(4) Li, J.; Liu, J.; Wu, Z.; Shang, X.; Li, Y.; Huo, W.; Huang, X. Fully printed and self-compensated bioresorbable electrochemical devices based on galvanic coupling for continuous glucose monitoring. *Sci. Adv.* **2023**, *9* (29), No. eadi3839.

(5) Dagdeviren, C.; Hwang, S. W.; Su, Y.; Kim, S.; Cheng, H.; Gur, O.; Haney, R.; Omenetto, F. G.; Huang, Y.; Rogers, J. A. Transient, biocompatible electronics and energy harvesters based on ZnO. *Small* **2013**, *9* (20), 3398−3404.

(6) Kang, S. K.; Murphy, R. K.; Hwang, S. W.; Lee, S. M.; Harburg, D. V.; Krueger, N. A.; Shin, J.; Gamble, P.; Cheng, H.; Yu, S.; et al. Bioresorbable silicon electronic sensors for the brain. *Nature* **2016**, *530* (7588), 71−76.

(7) Son, D.; Lee, J.; Lee, D. J.; Ghaffari, R.; Yun, S.; Kim, S. J.; Lee, J. E.; Cho, H. R.; Yoon, S.; Yang, S.; et al. Bioresorbable Electronic Stent Integrated with Therapeutic Nanoparticles for Endovascular Diseases. *ACS Nano* **2015**, *9* (6), 5937−5946.

(8) Lee, C. H.; Kim, H.; Harburg, D. V.; Park, G.; Ma, Y.; Pan, T.; Kim, J. S.; Lee, N. Y.; Kim, B. H.; Jang, K. I.; et al. Biological lipid membranes for on-demand, wireless drug delivery from thin, bioresorbable electronic implants. *NPG Asia Mater.* **2015**, *7*, No. e227, DOI: 10.1038/am.2015.114.

(9) Sun, J.; Wang, H.; Song, F.; Wang, Z.; Dang, B. J.; Yang, M.; Gao, H. X.; Ma, X. H.; Hao, Y. Physically Transient Threshold Switching Device Based on Magnesium Oxide for Security Application. *Small* **2018**, *14* (27), No. 1800945, DOI: 10.1002/smll.201800945.

(10) Durukan, M. B.; Cicek, M. O.; Doganay, D.; Gorur, M. C.; Çınar, S.; Unalan, H. E. Multifunctional and physically transient supercapacitors, triboelectric nanogenerators, and capacitive sensors. *Adv. Funct. Mater.* **2022**, *32* (1), No. 2106066.

(11) Ko, G.-J.; Han, S. D.; Kim, J.-K.; Zhu, J.; Han, W. B.; Chung, J.; Yang, S. M.; Cheng, H.; Kim, D.-H.; Kang, C.-Y.; Hwang, S. W. Biodegradable, flexible silicon nanomembrane-based NOx gas sensor system with record-high performance for transient environmental monitors and medical implants. *NPG Asia Mater.* **2020**, *12* (1), No. 71.

(12) Yu, X. W.; Shou, W.; Mahajan, B. K.; Huang, X.; Pan, H. Materials, Processes, and Facile Manufacturing for Bioresorbable

Electronics: A Review. *Adv. Mater.* **2018**, *30* (28), No. 1707624, DOI: 10.1002/adma.201707624.
(13) Tan, M. J.; Owh, C.; Chee, P. L.; Kyaw, A. K. K.; Kai, D.; Loh, X. J. Biodegradable electronics: cornerstone for sustainable electronics and transient applications. *J. Mater. Chem. C* **2016**, *4* (24), 5531−5558.
(14) Yin, L.; Cheng, H. Y.; Mao, S. M.; Haasch, R.; Liu, Y. H.; Xie, X.; Hwang, S. W.; Jain, H.; Kang, S. K.; Su, Y. W.; et al. Dissolvable Metals for Transient Electronics. *Adv. Funct. Mater.* **2014**, *24* (5), 645−658.
(15) Hwang, S. W.; Song, J. K.; Huang, X.; Cheng, H. Y.; Kang, S. K.; Kim, B. H.; Kim, J. H.; Yu, S.; Huang, Y. G.; Rogers, J. A. High-Performance Biodegradable/Transient Electronics on Biodegradable Polymers. *Adv. Mater.* **2014**, *26* (23), 3905−3911.
(16) Kang, S. K.; Park, G.; Kim, K.; Hwang, S. W.; Cheng, H. Y.; Shin, J. H.; Chung, S. J.; Kim, M.; Yin, L.; Lee, J. C.; et al. Dissolution Chemistry and Biocompatibility of Silicon- and Germanium-Based Semiconductors for Transient Electronics. *ACS Appl. Mater. Interfaces* **2015**, *7* (17), 9297−9305.
(17) Kang, S. K.; Koo, J.; Lee, Y. K.; Rogers, J. A. Advanced Materials and Devices for Bioresorbable Electronics. *Acc. Chem. Res.* **2018**, *51* (5), 988−998.
(18) Han, W. B.; Lee, J. H.; Shin, J. W.; Hwang, S. W. Advanced Materials and Systems for Biodegradable, Transient Electronics. *Adv. Mater.* **2020**, *32* (51), No. 2002211, DOI: 10.1002/adma.202002211.
(19) Huang, X.; Liu, Y.; Hwang, S. W.; Kang, S. K.; Patnaik, D.; Cortes, J. F.; Rogers, J. A. Biodegradable materials for multilayer transient printed circuit boards. *Adv. Mater.* **2014**, *26* (43), 7371−7377.
(20) Dahiya, A. S.; Zumeit, A.; Christou, A.; Dahiya, R. High-Performance n-Channel Printed Transistors on Biodegradable Substrate for Transient Electronics. *Adv. Electron. Mater.* **2022**, *8* (9), No. 2200098, DOI: 10.1002/aelm.202200098.
(21) Shou, W.; Mahajan, B. K.; Ludwig, B.; Yu, X. W.; Staggs, J.; Huang, X.; Pan, H. Low-Cost Manufacturing of Bioresorbable Conductors by Evaporation-Condensation-Mediated Laser Printing and Sintering of Zn Nanoparticles. *Adv. Mater.* **2017**, *29* (26), No. 1700172, DOI: 10.1002/adma.201700172.
(22) Huo, W. X.; Li, J. M.; Ren, M. N.; Ling, W.; Xu, H.; Tee, C. A. T. H.; Huang, X. Recent development of bioresorbable electronics using additive manufacturing. *Curr. Opin. Chem. Eng.* **2020**, *28*, 118−126.
(23) Lee, S.; Koo, J.; Kang, S.-K.; Park, G.; Lee, Y. J.; Chen, Y.-Y.; Lim, S. A.; Lee, K.-M.; Rogers, J. A. Metal microparticle−Polymer composites as printable, bio/ecoresorbable conductive inks. *Mater. Today* **2018**, *21* (3), 207−215.
(24) Mahajan, B. K.; Yu, X.; Shou, W.; Pan, H.; Huang, X. Mechanically Milled Irregular Zinc Nanoparticles for Printable Bioresorbable Electronics. *Small* **2017**, *13* (17), No. 1700065, DOI: 10.1002/smll.201700065.
(25) Yang, W. D.; Dong, Z. C.; Guo, Z. H.; Wang, C. H. Tailored Silver Malonate Conductive Ink with Tunable Performance Formulated from Mixed Silver Dicarboxylates. *ACS Appl. Electron. Mater.* **2023**, *5* (5), 2598−2607.
(26) Kalhori, A. H.; Kim, W. S. Printed Wireless Sensing Devices using Radio Frequency Communication. *ACS Appl. Electron. Mater.* **2023**, *5*, 1−10.
(27) Onses, M. S.; Sutanto, E.; Ferreira, P. M.; Alleyne, A. G.; Rogers, J. A. Mechanisms, Capabilities, and Applications of High-Resolution Electrohydrodynamic Jet Printing. *Small* **2015**, *11* (34), 4237−4266.
(28) Walker, S. B.; Lewis, J. A. Reactive silver inks for patterning high-conductivity features at mild temperatures. *J. Am. Chem. Soc.* **2012**, *134* (3), 1419−1421.
(29) Hassan, C. M.; Trakampan, P.; Peppas, N. A.Water Solubility Characteristics of Poly(vinyl alcohol) and Gels Prepared by Freezing/Thawing Processes. In *Water Soluble Polymers*; Springer, 2002; pp 31−40.
(30) Yoon, J.; Han, J.; Choi, B.; Lee, Y.; Kim, Y.; Park, J.; Lim, M.; Kang, M. H.; Kim, D. H.; Kim, D. M.; et al. Three-Dimensional Printed Poly(vinyl alcohol) Substrate with Controlled On-Demand Degradation for Transient Electronics. *ACS Nano* **2018**, *12* (6), 6006−6012.
(31) Park, J. C.; Ito, T.; Kim, K. O.; Kim, K. W.; Kim, B. S.; Khil, M. S.; Kim, H. Y.; Kim, I. S. Electrospun poly(vinyl alcohol) nanofibers: effects of degree of hydrolysis and enhanced water stability. *Polym. J.* **2010**, *42* (3), 273−276.
(32) Harpaz, D.; Axelrod, T.; Yitian, A. L.; Eltzov, E.; Marks, R. S.; Tok, A. I. Dissolvable polyvinyl-alcohol film, a time-barrier to modulate sample flow in a 3D-printed holder for capillary flow paper diagnostics. *Materials* **2019**, *12* (3), No. 343.
(33) Li, Y. M.; Zhang, Z. T.; Li, X. Y.; Zhang, J.; Lou, H. Q.; Shi, X.; Cheng, X. L.; Peng, H. S. A smart, stretchable resistive heater textile. *J. Mater. Chem. C* **2017**, *5* (1), 41−46.
(34) Avila, F. R.; McLeod, C. J.; Huayllani, M. T.; Boczar, D.; Giardi, D.; Bruce, C. J.; Carter, R. E.; Forte, A. J. Wearable electronic devices for chronic pain intensity assessment: A systematic review. *Pain Pract.* **2021**, *21* (8), 955−965.
(35) Bagherifard, S.; Tamayol, A.; Mostafalu, P.; Akbari, M.; Comotto, M.; Annabi, N.; Ghaderi, M.; Sonkusale, S.; Dokmeci, M. R.; Khademhosseini, A. Dermal Patch with Integrated Flexible Heater for on Demand Drug Delivery. *Adv. Healthcare Mater.* **2016**, *5* (1), 175−184.
(36) Hong, W.; Sun, B.; Li, Z.; Fu, Z.; Zhang, J.; Jiang, M.; Zhang, Y.; Li, Y.; Zhang, Y.; Qian, K. Biodegradable, Flexible Transparent Ordered Ag NWs Micromesh Conductor for Electrical Heater and Electromagnetic Interference Shielding Applications. *ACS Appl. Electron. Mater.* **2022**, *4* (11), 5446−5455.
(37) Sahin, F.; Pekdemir, S.; Sakir, M.; Gozutok, Z.; Onses, M. S. Transferrable SERS barcodes. *Adv. Mater. Interfaces* **2022**, *9* (17), No. 2200048.
(38) Lohse, D. Fundamental fluid dynamics challenges in inkjet printing. *Annu. Rev. Fluid Mech.* **2022**, *54*, 349−382.
(39) Celik, N.; Akay, S.; Sahin, F.; Sezer, G.; Dagasan Bulucu, E.; Ruzi, M.; Butt, H. J.; Onses, M. S. Sustainable and Practical Superhydrophobic Surfaces via Mechanochemical Grafting. *Adv. Mater. Interfaces* **2023**, *10*, No. 2300069.
(40) Stempien, Z.; Rybicki, E.; Rybicki, T.; Lesnikowski, J. Inkjet-printing deposition of silver electro-conductive layers on textile substrates at low sintering temperature by using an aqueous silver ions-containing ink for textronic applications. *Sens. Actuators, B* **2016**, *224*, 714−725.
(41) Gozutok, Z.; Kinj, O.; Torun, I.; Ozdemir, A. T.; Onses, M. S. One-step deposition of hydrophobic coatings on paper for printed-electronics applications. *Cellulose* **2019**, *26*, 3503−3512.
(42) Onses, M. S.; Song, C.; Williamson, L.; Sutanto, E.; Ferreira, P. M.; Alleyne, A. G.; Nealey, P. F.; Ahn, H.; Rogers, J. A. Hierarchical patterns of three-dimensional block-copolymer films formed by electrohydrodynamic jet printing and self-assembly. *Nat. Nanotechnol.* **2013**, *8* (9), 667−675.
(43) Zubair, N. A.; Rahman, N. A.; Lim, H. N.; Zawawi, R. M.; Sulaiman, Y. Electrochemical properties of PVA−GO/PEDOT nanofibers prepared using electrospinning and electropolymerization techniques. *RSC Adv.* **2016**, *6* (21), 17720−17727.
(44) Mansur, H. S.; Oréfice, R. L.; Mansur, A. A. Characterization of poly (vinyl alcohol)/poly (ethylene glycol) hydrogels and PVA-derived hybrids by small-angle X-ray scattering and FTIR spectroscopy. *Polymer* **2004**, *45* (21), 7193−7202.
(45) Krimm, S.; Liang, C.; Sutherland, G. Infrared spectra of high polymers. V. Polyvinyl alcohol. *J. Polym. Sci.* **1956**, *22* (101), 227−247.
(46) Mansur, H. S.; Sadahira, C. M.; Souza, A. N.; Mansur, A. A. P. FTIR spectroscopy characterization of poly (vinyl alcohol) hydrogel with different hydrolysis degree and chemically crosslinked with glutaraldehyde. *Mat Sci. Eng.: C* **2008**, *28* (4), 539−548.
(47) Wang, Q. W.; Zhang, H. B.; Liu, J.; Zhao, S.; Xie, X.; Liu, L. X.; Yang, R.; Koratkar, N.; Yu, Z. Z. Multifunctional and Water-Resistant

MXene-Decorated Polyester Textiles with Outstanding Electromagnetic Interference Shielding and Joule Heating Performances. *Adv. Funct. Mater.* **2019**, *29* (7), No. 1806819, DOI: 10.1002/adfm.201806819.

(48) Gozutok, Z.; Agırbas, O.; Bahtiyari, M. I.; Ozdemir, A. T. Low-voltage textile-based wearable heater systems fabricated by printing reactive silver inks. *Sens. Actuators, A* **2021**, *322*, No. 112610.

(49) Peçenek, H.; Dokan, F. K.; Onses, M. S.; Yılmaz, E.; Sahmetlioglu, E. Highly compressible binder-free sponge supercapacitor electrode based on flower-like NiO/MnO2/CNT. *J. Alloys Compd.* **2022**, *913*, No. 165053.

(50) Hasan, M. M.; Sadeque, M. S. B.; Albasar, I.; Pecenek, H.; Dokan, F. K.; Onses, M. S.; Ordu, M. Scalable Fabrication of MXene-PVDF Nanocomposite Triboelectric Fibers via Thermal Drawing. *Small* **2023**, *19* (6), No. 2206107.

(51) Tian, M. W.; Hao, Y. N.; Qu, L. J.; Zhu, S. F.; Zhang, X. S.; Chen, S. J. Enhanced electrothermal efficiency of flexible graphene fabric Joule heaters with the aid of graphene oxide. *Mater. Lett.* **2019**, *234*, 101−104.

https://doi.org/10.1021/acsaelm.4c00569
ACS Appl. Electron. Mater. 2024, 6, 5599−5607